A Coarse-Grained Model for Physical Behavior of Phosphorene Sheet

Journal:	*Physical Chemistry Chemical Physics*
Manuscript ID	CP-ART-11-2018-006918.R1
Article Type:	Paper
Date Submitted by the Author:	14-Dec-2018

Complete List of Authors:	Liu, Ning; University of Georgia, College of Engineering Becton, Matthew; University of Georgia, College of Engineering Zhang, Liuyang; Xi'an Jiaotong University Chen, Heng; Nanjing University of Aeronautics and Astronautics Zeng, Xiaowei; University of Texas at San Antonio, Department of Mechanical Engineering Pidaparti, Ramana; University of Georgia Wang, Xianqiao; University of Georgia, College of Engineering

A Coarse-Grained Model for Mechanical Behavior of Phosphorene Sheet

Ning Liu[1], Mathew Becton[1], Liuyang Zhang[2], Heng Chen[3], Xiaowei Zeng[4], Ramana Pidaparti[1] and Xianqiao Wang[1*]

[1]College of Engineering, University of Georgia, Athens, GA 30602 USA

[2] State Key Laboratory for Manufacturing Systems Engineering, Xi'an Jiaotong University, Xi'an, Shaanxi, 710049, China

[3]College of Astronautics, Nanjing University of Aeronautics and Astronautics, Nanjing, 210016, China

[4]Department of Mechanical Engineering, University of Texas at San Antonio, San Antonio, TX 78249 USA

[*]Corresponding author: xqwang@uga.edu

Abstract

The popularity of phosphorene (known as monolayer black phosphorous) in electronic devices relies on not only its superior electrical properties but also its mechanical stability beyond nanoscale. However, the mechanical performance of phosphorene beyond nanoscale remain poorly explored owing to spatiotemporal limitation of experimental observations, first-principle calculations, and atomistic simulations. To overcome this limitation, here a coarse-grained molecular dynamics (CG-MD) model is developed via a strain energy conservation approach to offer a new computational tool for the investigation of the mechanical properties of phosphorene beyond nanoscale. Mechanical properties of a single phosphorene sheet are first characterized by all-atom molecular dynamics (AA-MD) simulations, followed by a force-field parameter optimization of CG-MD model by matching these mechanical properties from AA-MD simulations. The intrinsic out-of-plane puckered feature is conserved in our CG-MD model, rendering mechanical anisotropy and heterogeneity in both in-plane and out-of-plane directions persevered. Results indicate that our coarse-grained model is able to accurately capture the anisotropic in-plane mechanical performance of phosphorene and quantitatively reproduce Young's modulus, ultimate strength, and fracture strain under various environmental temperatures. Our CG-MD model can also capture the anisotropic out-of-plane bending stiffness of phosphorene. We demonstrate the applicability of our model in capturing the fracture toughness of phosphorene in both armchair and zigzag directions by comparing results from AA-MD simulations. This CG-MD model proposed here offers greater capability to perform mechanical mesoscale simulations for phosphorene-based systems, allowing for a deeper understanding of the mechanical properties of phosphorene beyond nanoscale, and the potential transferability of the developed force-field can help design hybrid phosphorene devices and structures.

Keywords: phosphorene, coarse-grained, strain energy, force-field, fracture, toughness

1. Introduction

Recent years have witnessed the explosive development in two-dimensional materials with one-atom thickness, which have shown their great potential in many nanotechnology applications. Phosphorene, a single layer of black phosphorus, is one of the good examples, which has multiple unique physical properties, such as layer-dependent direct band gap and high carrier mobility as predicted by theories and validated by experiments [1, 2]. In terms of applications, its mechanical performance would be critical for robustness and reliability of nanodevices made from phosphorene. It has been revealed that the puckered structure of phosphorene endows it multiple unique mechanical properties, such as anisotropic elastic moduli [3-7] and negative Poisson's ratio [8]. However, the underlying mechanism of the above mechanical phenomena remains largely unexplored. On one hand, due to the spatiotemporal limitations of experimental observations, limited insight has been offered into the molecular scale processes in the pursue of intriguing mechanical properties of phosphorene. On the other hand, first principle or atomistic simulations of large-size phosphorene sheets beyond nanoscale are computationally expensive and demanding. As we know, coarse-grained molecular dynamics (CG-MD) simulations, in which a small cluster of atoms are united as a mass point, shows its great potential in overcoming the spatial and temporal limitations for studying the mechanical properties of two-dimension materials [9-12]. Following this vein, this paper will develop a CG model of phosphorene sheets to investigate the mechanical properties of phosphorene, which may also help design hybrid phosphorene structures with synthetic polymers due to great transferability of the developed force-field potential.

In order to address the scale-related issue and gain a comprehensive physical understanding of large-size phosphorene sheets, it is noteworthy to briefly review and discuss these findings from the current atomistic simulations. As we know, most prior investigations on phosphorene modeling were carried out using all-atom atomistic (AA-MD) simulations or first principles calculations, which provides valuable insights into molecular mechanisms governing constitutive behavior while retaining critical chemical details [4, 6, 13-19]. Despite tremendous success in understanding and predicting the mechanical behaviors of phosphorene through AA-MD simulations, there still exists challenging problems for these computational approaches to be tackled. The most critical one is the temporal and spatial scale of AA-MD simulations as these approaches are extremely demanding in computational cost. In order to facilitate phosphorene simulations that reach a larger scale in both time and space, an upscaling computational technique is required. CG-MD simulations aiming at predicting the key properties of nanomaterials offer insights into the molecular scale dynamic processes over extended scales and increase computational efficiency dramatically compared to AA-MD simulations. For instance, a CG model for graphene developed recently can achieve about 200-fold increase in computational speed

compared with AA-MD simulations, which can also capture the mechanical properties of graphene, such as non-linear elasticity at large deformation, fracture strength, and orientation-dependent interlayer shear responses [20]. Close agreement between simulation results and experimental data indicates the applicability of CG-MD modeling to understand mechanical properties of nanomaterials.

CG-MD has been extensively employed to study a variety of problems involving 2D materials, such as graphene-lipid membrane interactions [21], folding mechanics of graphene [10], nacre-inspired polymer composites [22, 23] and spalling like failure of mesoscale membranes [11, 24] . However, to the best of our knowledge, there is no reliable CG models for phosphorene yet, which is essential in exploration of its potential applications similar as graphene aforementioned from the simulation perspective. There are two major approaches, namely parametrized and derived coarse-graining methods, to develop an effective CG-MD model. In the parameterized methods, AA-MD simulations or first-principle calculations are performed first to obtain target properties, such as pair distribution function or force distribution function, and then the CG model is constructed to reproduce these properties via optimization. An exemplar is called iterative inverse Boltzmann inverse method (IBM) [25], which aims to reproduce the target pair distribution functions given by AA-MD simulations. This approach has been widely used in the development of CG models for synthetic polymers [26, 27]. In the derived CG methods, direct all-atom simulations are employed between the super-atoms to derive the interactions accordingly, in which the target properties are not reproduced but predicted by the CG-MD model [28-30]. For phosphorene, a combination of parameterized and derived CG methods should help facilitate the construction of the coarse-grained model, in which the anisotropic elastic moduli [31] could be derived through force calculation while the non-linear mechanical responses at large strain [32] can barely be reproduced without the force-displacement profile from AA-MD simulations.

Our CG-MD model will be constructed via a strain energy conservation approach, similar as parameterized CG method, inspired by the previous CG models for graphene-based materials. In this paper, we first provide a description of the CG model of phosphorene and characterize its atomistic properties using AA-MD simulations, followed by calibrating the force-field parameters using the CG model via optimization. Next, we compare the mechanical properties of phosphorene from both CG-MD and AA-MD simulation results. Finally, we demonstrate the applicability of the model by measuring the fracture toughness of a monolayer phosphorene sheet. Our CG-MD model results agree reasonably well with results from first principle calculations and AA-MD simulations.

2. Methods and Models

2.1 CG-MD Model Description

In this paper, we employ a coarse-grained (CG) bead-spring network to model the pristine phosphorene, in which four adjacent phosphorene atoms are grouped into one single bead as shown in Figure 1(a). This CG level is in accordance with commonly used approaches, such as Martini model for polymers and CG model of graphene [20, 26, 33-35], rendering our model compatible with existing models for polymers and other 2D materials. Figure 1(b) shows a unit cell of the model while Figure 1(c) shows the overall view of the model from different perspectives, in which the out-of-plane puckered feature of phosphorene sheets is reserved to accurately depict its mechanical anisotropy. Note that the bonds and angles on different orientations, armchair and zigzag, are differentiated as shown in Figure 1(b). In this model, bonded covalent interactions inside a single phosphorene sheet are modeled as explicit bonds and angles among adjacent coarse-grained beads while non-bonded van der Waals forces between neighboring phosphorene sheets are captured by a 12-6 Lennard-Jones (LJ) potential. For both bond and bond-angle potentials here, Morse bond potentials [35, 36] instead of conventional harmonic potentials are chosen to capture nonlinear mechanical responses of phosphorene sheets. The total potential energy of the system can be written as:

$$U_p = U_{b1} + U_{b2} + U_{\theta 1} + U_{\theta 2} + U_{nb} \tag{1}$$

where U_{b1}, U_{b2}, $U_{\theta 1}$, $U_{\theta 2}$ and U_{nb} are the sum over the energies of type 1 bond, type 2 bond, type 1 angle, type 2 angle and non-bonded interactions. The detailed formula for each specific term of potential energy in Eq. (1) are shown as follows:

$$U_{b1}(d_1) = D_{11}[1 - e^{-\alpha_{11}(d_1 - d_1^0)}]^2 \tag{2}$$

$$U_{b2}(d_2) = D_{12}[1 - e^{-\alpha_{12}(d_2 - d_2^0)}]^2 \tag{3}$$

$$U_{\theta 1}(\theta_1) = D_{21}[1 - e^{-\alpha_{21}(\theta_1 - \theta_1^0)}]^2 \tag{4}$$

$$U_{\theta 2}(\theta_2) = D_{22}[1 - e^{-\alpha_{22}(\theta_2 - \theta_2^0)}]^2 \tag{5}$$

$$U_{nb}(r) = 4\varepsilon[(\frac{\sigma}{r})^{12} - (\frac{\sigma}{r})^{6}] \tag{6}$$

where D_{ij} and α_{ij} (i, j =1, 2) are the depth and a parameter related to the width of the potential well of the bond (angle), respectively, d_i^0 (i = 1, 2) is the equilibrium distance of bond, θ_i^0 (i = 1,2) is the equilibrium angle, ε is the depth of the LJ potential well for non-bonded interactions and σ is related to the equilibrium distance (r_0) between two non-bonded beads from different phosphorene sheets ($r_0 = 2^{\frac{1}{6}}\sigma$). There are 14 independent parameters in this entire potential system, in which d_i^0, θ_i^0 (i = 1, 2) and σ can be determined from the equilibrium geometrical configuration of phosphorene. For the current model: $d_1^0 = 4.16$ Å, d_2^0

=4.12 Å, θ_1^0 = 114.2°, θ_2^0 = 83.8° and σ = 4.45 Å are obtained to ensure that the interlayer distance h is equal to 5.24 Å as shown in Figure 1(d) [7, 37]. Therefore, there are 9 parameters left that require calibration (D_{ij}, α_{ij} and ε (i, j = 1, 2)) in order to reproduce the mechanical properties of phosphorene.

2.2 CG-MD model calibration

The essence of our CG-MD model is to capture the mechanical behavior of phosphorene sheets. As pointed in continuum mechanics, the mechanical constitutive properties of a material heavily depends on its strain energy density function [38], therefore, a strain energy conservation approach is deployed here to calibrate the above parameters. Targeted mechanical properties of phosphorene, such as elastic modulus and fracture strain, were obtained from both all-atom atomistic simulations and relevant data from the literature [3-7, 39]. These corresponding values are listed as follows: elastic modulus equal to 38.5 (armchair) and 145.0 GPa (zigzag), and fracture strain equal to 0.32 (armchair) and 0.58 (zigzag) [7]. Reactive Force Field (ReaxFF) [7] was implemented to perform AA-MD simulations due to its accurate description of chemical and mechanical properties of phosphorene. First of all, it is important to establish the relationship between bond and angle stiffness in the CG-MD model and the in-plane elastic moduli of pristine phosphorene. Towards this purpose, two typical scenarios are picked out, namely uniaxial tension in the armchair and zigzag directions as shown in Figure 2. To simplify the derivation, stiffness of different types of bonds (angles) are assumed to be identical to each other, which would result in the following formula:

$$\begin{pmatrix} \cos^2(32.9^0) + \frac{\cos^2(79.8^0)}{2} & \frac{\sin^2(32.9^0)(d_1^0)^2}{4c_3} + \frac{\sin^2(79.8^0)(d_2^0)^2}{4c_1 + 4c_2} \\ 2\cos^2(32.9^0) & \frac{\sin^2(32.9^0)(d_2^0)^2}{2c_4} \end{pmatrix} \begin{Bmatrix} \frac{1}{k_d} \\ \frac{1}{k_\theta} \end{Bmatrix} = \begin{Bmatrix} \frac{a_1}{2a_2 h E_{arm}} \\ \frac{2a_2}{a_1 h E_{zig}} \end{Bmatrix} \tag{7}$$

The derivation and detailed explanation of Eq.7, following a similar procedure developed by Gillis et al [40] in which 2D materials are considered as a spring network, can be found in the Supplemental Materials. Solving Eq. 7 results in the magnitude of stiffness of bonds and angles, k_d and k_θ, which are 9.73 eV/Å^2 and 13.07 eV/radian^2, respectively. The relation between stiffness of above springs and parameters in Eqs. (2)-(5) are expressed in the following formula:

$$k_d = 2D_{11}{\alpha_{11}}^2 = 2D_{12}{\alpha_{12}}^2 \tag{8}$$

$$k_\theta = 2D_{21}{\alpha_{21}}^2 = 2D_{22}{\alpha_{22}}^2 \tag{9}$$

It is worth noting that there are still four independent parameters left for bonds and angles in the CG-MD model, which are difficult to be calibrated simultaneously. Therefore, we calibrated them sequentially and started from parameters (D_{11},D_{12}, α_{11} and α_{12}) regarding bonds first. The primary target of the current optimization step is to make a close match to elastic moduli and a rough estimation of fracture strain.

Therefore, to reduce the number of independent variables, we use harmonic angles with fixed spring constant equal to k_θ to represent Morse potential angles. The Morse potential angles would behave like harmonic angles when the variation of angle is small. Therefore, this does not change the final results regarding elastic moduli, but only enhances the ease of calculation. The parameters involved in the Morse angle potential would be optimized in the following step in order to match the fracture strain and ultimate strength from AA-MD. AA-MD simulations were performed to provide reference for our calibration. As we can see from Figure 3(a), the fracture strain in the armchair direction is around 0.57 while in the zigzag direction it is around 0.32. In our CG-MD model, fracture strain can be tuned through varying the magnitude of α. According to a previous study, α is set to 1.55 $Å^{-1}$ in the CG-MD model of graphene and the resultant fracture strain is 0.16 [20]. Therefore, α_{11} and α_{12} are both set to 0.775 $Å^{-1}$, half of that in CG-MD graphene model, in order to match the fracture strain of phosphorene. Note that the above determination of the parameters is just an estimation because the relation between α_{ij} and fracture strain is not exactly linear. CG-MD simulations of phosphorene are performed using aforementioned parameters, which are also shown in Figure 3(a). It turns out that the CG-MD model (marked as CG beta) can match well with the Reaxff model on the armchair direction while it fails to match on the zigzag direction in terms of fracture strain and ultimate strength, which is a good starting point for parameter calibration.

Next, parameter optimization is done sequentially through a trial-and-error approach to match the mechanical performance, namely fracture strain and ultimate strength, on both armchair and zigzag directions from AA-MD simulations. Note that stiffness of both bonds and angles, namely k_d and k_θ, varies subtly around its initial value during the calibration. First, α_{ij} are optimized in order to match the fracture strain from AA-MD simulations. Subsequently, D_{ij} are tuned in order to arrive a good agreement with ultimate strength from AA-MD simulations. The final parameters involved in the CG-MD model are listed in Table 1 for reference (marked as CG). Note that the bonds involved in this model are breakable while associated angles would be broken accordingly if bonds are broken, in which the cutoff distance for armchair and zigzag bonds is 5.4 and 4.8 Å, respectively, as listed in Table 1. However, the CG-MD model does not support bond formation based on inter-bead distance, in which the topological information for bonds and angles should be predefined. With the current set of parameters, the CG model shows good prediction accuracy of mechanical properties, including elastic modulus, fracture strain, and ultimate strength. It would be interesting how the final parameters would change if the optimization sequence is changed, which would be a possible research topic in future.

After calibration of parameters involved in bonded interactions, the only unknown parameter left in the CG-MD model is the depth of the LJ potential well for non-bonded interactions, ε, which determines the adhesion energy for phosphorene, γ_{ad}. In this work, we choose our target adhesion energy γ_{ad} = 0.345 J/m^2

as obtained in our previous work using AA-MD simulations [19]. Details about how the adhesion energy is calculated using our CG-MD model can be found in Figure S4 in the supplemental material. The optimized value for ε is equal to 0.167 eV as listed in Table 1.

2.3 CG-MD simulation protocols

All the CG-MD simulations are carried out using molecular dynamics (MD) package LAMMPS [41]. In MD simulations, time step is a key parameter for accuracy and stability, which should be small enough so that the fastest vibrational process should be sufficiently sampled. In our case, that should be the vibration of bonds connected adjacent beads. If considered as a harmonic oscillator, the angular frequency should be $\omega = \frac{2\pi}{T} = \sqrt{\frac{k}{m}}$, where k is the spring constant of bond while m is the mass of a single bead. It is widely accepted by the community that the time step $\Delta t < T/10$, where T is the period of the oscillator. Therefore, in this case, the upper bound for time-step is around 26.9 fs. A sensitivity analysis revealed that the time-step can be pushed up to 20 fs with good stability if a very big system is considered. For a better stability and accuracy, we choose 5 fs as the time step in simulations hereafter if not specified.

In order to calibrate the in-plane mechanical responses of the CG-MD model, a periodic single sheet of phosphorene with dimensions 20 nm×20 nm in the $x-y$ plane is used in simulations while the material orientation θ of the model can be changed from 0^o (armchair) to 90^0 (zigzag) as shown in Figure 3(b), in which the arrow represents the armchair direction while the dashed line represents the x axis in the coordinate system. The system was first energy minimized and then equilibrated in the NPT ensemble at temperature 1K for 20,000 time steps. After the equilibration, the sample was then stretched uniaxially along the x-direction using a strain-controlled loading method, in which the deformation is added every 2,000 time steps by deforming the simulation box, and the equivalent strain rate is around 1×10^8 s^{-1}. Subsequently, the environmental temperature is changed from 1 to 400 K to test the mechanical properties accordingly. AA-MD simulations are also performed as a control, in which similar simulation setup is adopted except that the time step is 1 fs.

To measure the out-of-plane bending stiffness, a finite-sized single sheet with dimensions 20 nm×20 nm is used. Virtual cylinders with different radii are chosen to create deformation patterns with different curvatures, in which the phosphorene was adhered to the surface of the associated cylinders through LJ interactions between them. After the deformation patterns was constructed, the virtual cylinders were removed, four edges of phosphorene sheets were fixed, and the remaining parts of the sheet were allowed to relax until the energy is minimized, energy fluctuation being smaller than 5 percent of the total energy. In order to test that the constraints at the sheet boundaries have small effects, we performed simulations where only the 2 straight edges of the sheet were constrained and the bended edges of the sheet were set

free. We observed that the energy of the system is almost identical to the case where all the edges are fixed, suggesting that the boundary conditions have minimal impact on the energy of the system as long as the system is minimized in the deformed state.

Finally, we apply our CG-MD model to study the fracture toughness of phosphorene sheets with different crack lengths. The same dimension size as the uniaxial tension case is used. A central crack with different lengths in the samples is generated by deleting beads and corresponding bond and angle interactions along a set path. The cracks are aligned with the zigzag direction and tensile loading is applied in the armchair direction for simulation tests in Figure 6. An equivalent deformation procedure to that used in uniaxial tensile deformation is applied. Similar results with cracks aligned with the armchair direction and tension along the zigzag direction can be found in Figure S4.

Results and Discussions

One of the most intriguing mechanical properties of phosphorene is its mechanical anisotropy [17]. As we can see in the Figure 3(a) , the mechanical responses to the two characteristic material directions, namely armchair and zigzag directions, are obviously different, in which phosphorene is ductile and soft in the armchair direction while it is stiff and brittle in the zigzag direction. As intensively discussed in previous studies, phosphorene is highly anisotropic, in which the elastic modulus in the zigzag direction is much higher than that in the armchair direction while the ultimate strength in the zigzag direction is much lower [4, 6, 16, 17, 31, 37]. This intrinsic chiral dependence of phosphorene can be attributed to its unique puckered structure. When stretched in the armchair direction, the puckered phosphorene sheet flattens with moderate changes in the bond lengths, resulting in relatively low elastic modulus but high ultimate strength [6]. However, when strain is applied in the zigzag direction, the bonds, namely b2 bond in our model, experience significant changes, leading to a relatively high Young's modulus but low strength [17]. As we can see in Figure 3, our parameterized CG-MD model well reproduces the anisotropy of phosphorene, which results from the preserve of the intrinsic puckered honeycomb structure in the CG-MD model. Note that the difference between Reaxff model and CG model is marginal, indicating high accuracy of our proposed CG-MD model in reproducing mechanical properties of phosphorene. It is worth noting that the good agreement with AA-MD in highly non-linear regime is also achieved due to the anharmonic Morse bond and angle potentials [20].

Thanks to the huge differences in elastic modulus between the armchair and zigzag directions, phosphorene sheets exhibit super stiffness tunability, which could be an ideal material in large-strain engineering applications [42-46]. Therefore, in order to explore unprecedented opportunities in phosphorene applications, it is computationally crucial for a CG-MD model of phosphorene able to reproduce its super mechanical flexibility. Results from both Reaxff model and our CG-MD models show that elastic moduli

increase as θ increases since the phosphorene sheet transits from the softer armchair direction to the stiffer zigzag direction [6]. The material orientation θ is defined as the angle between loading direction and armchair direction as shown in inset of Figure 3(b). These results of our developed CG-MD model in Figure 3(b) demonstrate its robustness in studying the mechanical tunability of phosphorene.

As it is claimed in the literature [13, 16, 17, 19, 47], the mechanical properties of 2D materials, and phosphorene in particular, are highly sensitive to temperature. Therefore, it is important for a CG-MD model able to capture the temperature dependence of mechanical properties of phosphorene. For both CG-MD and AA-MD model, the temperature and pressure were controlled via NPT ensemble. Figure 4 shows the stress-strain responses for both ReaxFF model and CG-MD model (CG). The mechanical responses of CG-MD model (CG) are very similar to the counterpart using AA-MD model based on ReaxFF potential. For further analysis, both elastic moduli and ultimate strength are plotted as a function of temperature. As shown in Figure 5(a), the elastic modulus undergoes moderate alterations in both CG model and ReaxFF model. In contrast, the ultimate strength decreases as temperature increases as shown in Figure 5(b), recapturing similar patterns as discussed in previous literature [13, 16]. This temperature-induced strength reduction can be attributed to stronger thermal vibrations of atoms at a higher temperature. According to the Arrhenius equation, the reaction rate increases as the temperature increases. Physically speaking, with high translational energy at high temperature, phosphorus atoms can easily overcome the activation energy and break the bonds, leading to a much lower strength. Overall, results from our CG-MD model are very close to those from AA-MD model based on ReaxFF potential. However, we should admit that CG-MD model has some intrinsic limitations in predicting all mechanical properties accurately in a wide range of temperature, known as temperature transferability, due to its reduced degree of freedom caused by using a united mass point to represent a cluster of particles [27, 30, 48-50]. The temperature transferability problem of CG-MD models could be attributed to a variety of factors, including altered dynamics, underestimated viscosity, and imperfect thermal expansion due to both reduced degrees of freedom and utilization of attenuated pair potential to represent many-body interactions in AA-MD model [26, 27, 51, 52], which may not hold true for phosphorene. For instance, viscous forces or friction does not play an important role in determining the mechanical properties of phosphorene, in which bond and angle interactions are conserved instead of dissipative. Some limitations, however, are intrinsic due to the reduced degree of freedoms in CG-MD model, such as altered dynamics [51], which could be amended by adding extra friction to slow down the dynamics. Similar approaches include Langevin thermostat and dissipative particle dynamics [53, 54], which could help improve the temperature transferability of the parameterized CG-MD model in future.

Bending stiffness of 2D materials like phosphorene is very important from the perspective of applications such as strain engineering in which the electronic properties are tuned through applying an external strain

[55]. Although it is yet to be well predicted through conventional continuum theory even with known in-plane Young's modulus [55], the bending stiffness of 2D materials is an indispensable mechanical property. Owing to its puckered structure, phosphorene shows anisotropy in its bending stiffness, which is different from other 2D planar materials[55, 56]. Therefore, it is vital to evaluate the prediction accuracy of our CG-MD model in bending stiffness despite its high accuracy in predicting in-plane elastic modulus. CG-MD simulations are carried out to test the out-of-plane stiffness on both armchair and zigzag directions. Basically, several pure bending deformation patterns with different curvatures, ranging from 0.05 to 0.2 nm^{-1}, are applied to a single layer phosphorene sheet. Subsequently, the phosphorene sheet is allowed to relax with the fixed curvature applied and bending energy per unit area U will be measured. According to the theory of elasticity, within the linear regime the relations between the bending curvature and bending energy can be expressed as follows,

$$U = \frac{1}{2} D \kappa^2 \tag{10}$$

where D is bending stiffness on a given orientation of bending. By fitting the data points with Eq. (10), the bending stiffness D can be obtained. Relevant results from the literature and our work are summarized in Table 2. It can be seen that the bending stiffness along the zigzag direction is much higher than that along the armchair direction, resulting from differences in the in-plane stiffness along those two orientations. Also, it can be seen that the bending stiffness from our work falls into the range of the corresponding value from the previous literature for both armchair and zigzag directions. Unlike CG-MD models for graphene [10, 20, 21, 33], there is no separate dihedral potential term in our CG-MD model for phosphorene due to the unique puckered structure of phosphorene. Graphene, with a planar honeycomb structure, cannot exhibit its bending stiffness without an extra dihedral potential, in which the atom bond and angles experience marginal variance under bending. However, phosphorene, with a two-layer puckered hexagonal structure, can well describe its bending stiffness with just bond and angle potentials, in which atoms in different layers experience different deformation, namely compression and tension, under bending. In other words, unlike other planar 2D materials, the in-plane elastic modulus and out-of-plane bending stiffness are highly correlated for phosphorene, and our CG-MD model can well reproduce bending stiffness without a systematic calibration of dihedral potential, which may be also valid for other puckered 2D materials. Therefore, our strategy in treating bending stiffness of phosphorene could also offer new avenue for the development of CG models of other 2D materials with intrinsic puckered structurer, such as borophene [57].

As discussed in the literature, mechanical fracture of two-dimensional materials such as graphene could be described by classic Griffith theory applicable for brittle materials [58]. Classic brittle fracture has been

successfully studied via atomistic simulations [58, 59], in contrast with ductile and quasi-brittle materials, such as metals and polymeric materials, for which fracture mechanics are difficult to simulate in atomistic simulations as a result of a large plastic zone or process zone [60, 61]. In order to further validate our CG-MD model, here we measure the critical stress intensity factors of phosphorene in both armchair and zigzag directions, K_{I-arm} and K_{I-zig} which govern the linear-elastic fracture toughness of the material. Meanwhile, AA-MD simulations are also performed for comparison. According to Griffith theory, the critical nominal stress σ_c to induce crack propagation is a function of the crack length $2a$ for a film with a central penetrating crack as follows,

$$K = \sigma_c\sqrt{\pi a} = \sqrt{2\gamma E} \tag{11}$$

where γ is the surface energy, *i.e.*, edge energy for 2D materials, and E is the Young's modulus along the loading direction.

In order to obtain K_{I-arm} and K_{I-zig}, uniaxial tensile tests are performed for phosphorene sheets with different crack lengths, which is schematically shown in the inset of Figure 7. As shown in Figure 7, σ_c decreases as the crack length increases and the relation between those two quantities can be fitted well by Eq. (11) for both AA-MD and CG-MD simulations. Moreover, the difference is marginal between AA-MD and CGMD simulations in terms of stress intensity factors (K_{I-arm}^{CG-MD}= 13.01 GPa.nm$^{-0.5}$, K_{I-arm}^{AA-MD}= 11.21 GPa.nm$^{-0.5}$). Similar results for samples with cracks aligned with the armchair direction can be found in Figure S5. This perfect agreement between our CG-MD model and AA-MD model again affirms the robustness and feasibility of our CG-MD model in predicting mechanical properties of phosphorene system.

Conclusions

In this work, we present a CG-MD model of phosphorene which is capable of reproducing its mechanical properties, such as Young's moduli, out-of-plane bending stiffness, and fracture toughness. We employ a strain energy conservation approach to calibrate the potential parameters of CG-MD model according to AA-MD calculations via a reactive force field. Despite the simplicity of the force-field and the fact that the model is only calibrated according to two typical cases: uniaxial tension in both armchair and zigzag directions, we demonstrate that our model can quantitatively capture the Young's modulus, uniaxial tensile strength and interlayer adhesion energy. After validating our CG-MD model, we investigate the mechanical response of monolayer phosphorene under different temperatures ranging from 1 to 400 K, and show that the differences between AA-MD and CG-MD simulations are marginal. We also apply the CG-MD model to measure the fracture toughness of phosphorene sheets, and the results show that fracture toughness in both armchair and zigzag directions from our CG-MD model are in good agreement with those from AA-

MD simulations using a reactive force field. These analyses illustrate the capability of our CG-MD model in capturing mesoscale large-deformation and failure mechanisms. Our work sets the stage for future studies on the role of heterogeneity on the mechanical properties of multilayer phosphorene sheets and has the potential to shed key insights into failure mechanisms pertaining to phosphorene-based nanocomposites.

Acknowledgements

N.L., X.W, and R.P. acknowledge the support from the National Science Foundation (Grant No. CMMI-1610812). HC appreciates the support from the Basic Research Program (Natural Science Foundation) of Jiangsu Province (Grant No. BK20180417) (China) and China Postdoctoral Science Foundation (Grant No. 2018M630551). L.Y. Zhang appreciates the support from the National Natural Science Foundation of China (NSFC) under the grant No. 31741043 and No. 51805414. Computational simulations are performed at the UGA Advanced Computing Resource Center.

Tables

Table 1 Parameters involved in the CG-MD potential of phosphorene.

Connection type	Analytical expression	Parameters
Bond 1	$U_{b1}(d_1) = D_{11}[1 - e^{-\alpha_{11}(d_1 - d_1^0)}]^2$ for $d_1 < d_1^{cut}$	$D_{11} = 8.88\ eV$ $\alpha_{11} = 0.55\ \text{Å}^{-1}$ $d_1^0 = 4.16\ \text{Å}$ $d_1^{cut} = 5.40\ \text{Å}$
Bond 2	$U_{b2}(d_2) = D_{12}[1 - e^{-\alpha_{12}(d_2 - d_2^0)}]^2$ for $d_2 < d_2^{cut}$	$D_{12} = 5.52\ eV$ $\alpha_{12} = 0.80\ \text{Å}^{-1}$ $d_2^0 = 4.12\ \text{Å}$ $d_2^{cut} = 4.80\ \text{Å}$
Angle 1	$U_{\theta 1}(\theta_1) = D_{21}[1 - e^{-\alpha_{21}(\theta_1 - \theta_1^0)}]^2$	$D_{21} = 10788.2\ eV$ $\alpha_{21} = 0.022\ radian^{-2}$ $\theta_1^0 = 114.2^0$
Angle 2	$U_{\theta 2}(\theta_2) = D_{22}[1 - e^{-\alpha_{22}(\theta_2 - \theta_2^0)}]^2$	$D_{22} = 20396.5\ eV$ $\alpha_{22} = 0.016\ radian^{-2}$ $\theta_2^0 = 83.8^0$
Non-bonded	$U_{nb}(r) = 4\varepsilon[(\frac{\sigma}{r})^{12} - (\frac{\sigma}{r})^{6}]$ for $r < r_{cut}$	$\varepsilon = 0.167\ eV$ $\sigma = 4.45\ \text{Å}$ $r_{cut} = 13.5\ \text{Å}$

Table 2 Comparison between results about bending stiffness in the literature.

	Armchair D_{arm} (eV)	Zigzag D_{zig} (eV)
VFM [62]	1.1	7.4
DFT [56]	4.3	8.6
DFT [55]	3.3	8.2
MD [13]	6.5	8.8
This work	1.6	6.8

Figures

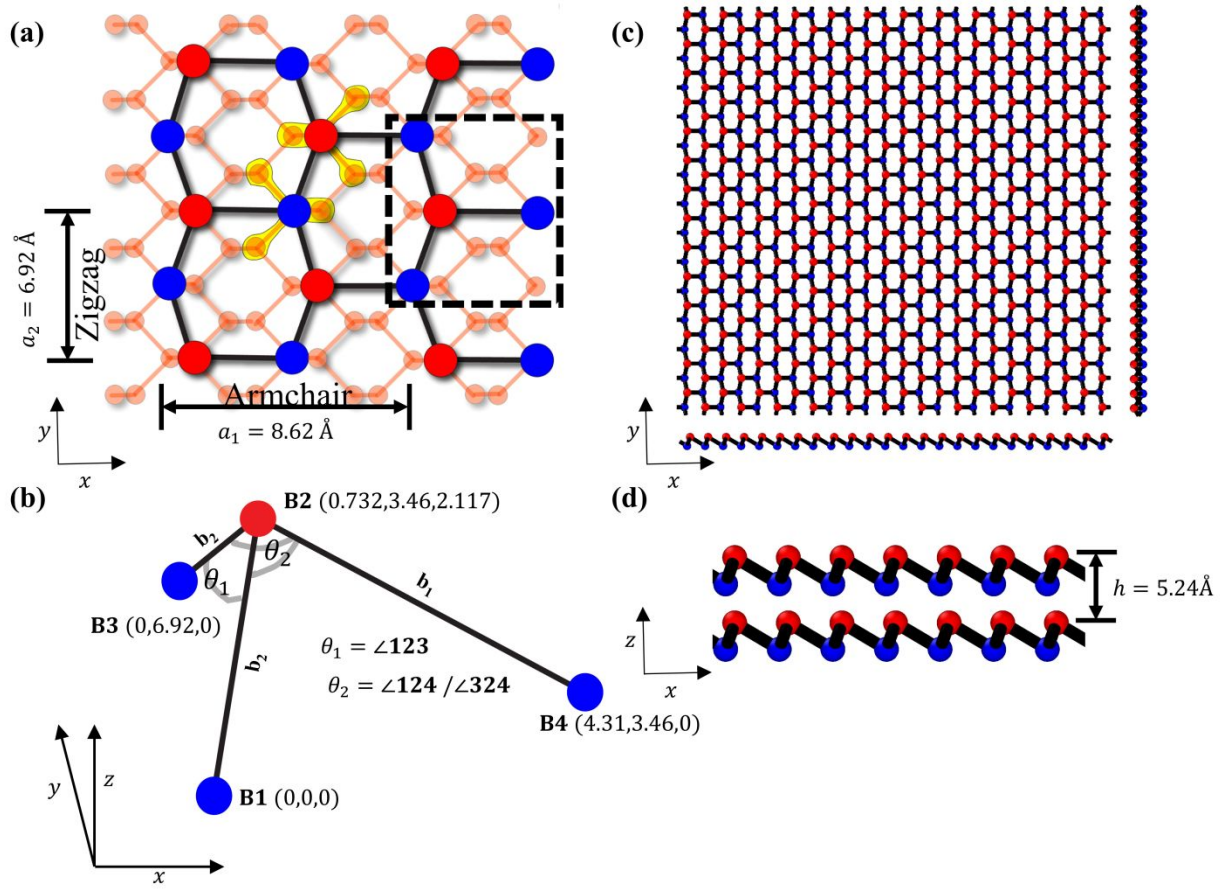

Figure 1. (a) Coarse-grained map of phosphorene (Top view); (b) Perspective view of the part marked by square in Figure 1(a); (c) Overview of single-layer coarse-grain model of phosphorene; (d) Interlayer distance of multilayer phosphorene.

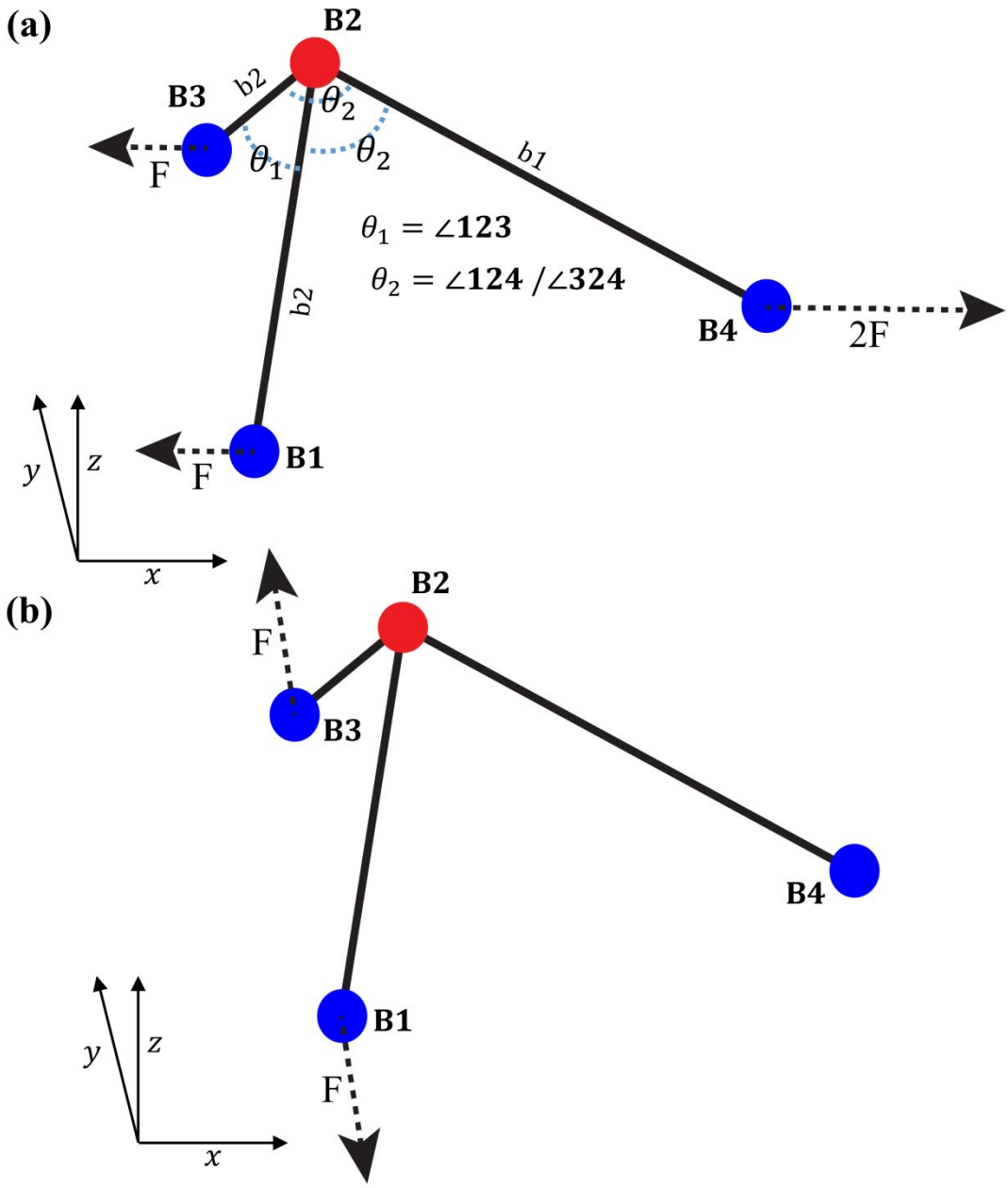

Figure 2. (a) Free body diagram of the unit cell under armchair uniaxial tension; (b) Free body diagram of the unit cell under zigzag uniaxial tension.

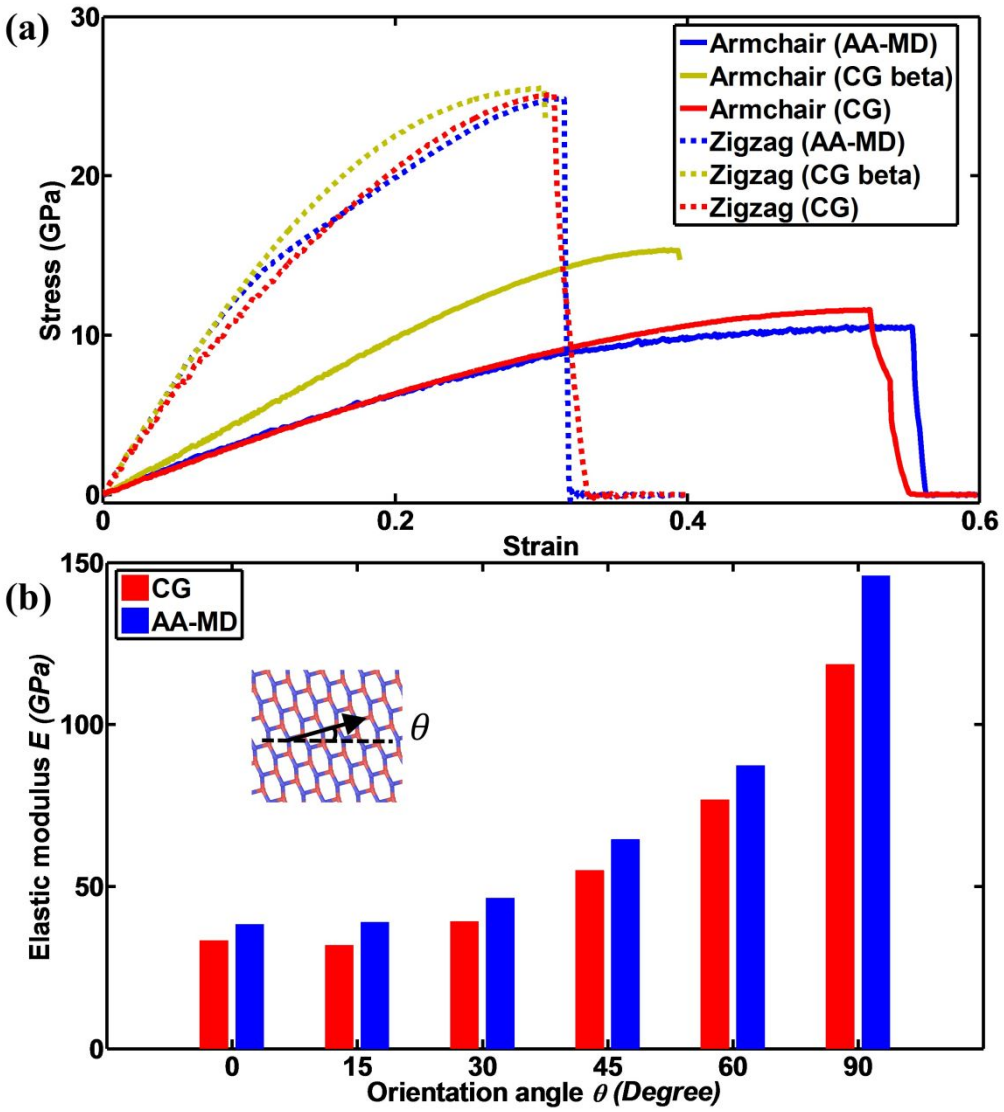

Figure 3. (a) Comparison of stress-strain responses regarding uniaxial tensile tests between CG-MD model and AA-MD model based on Reactive force field; (b) Comparison of elastic moduli on different material orientation between CG-MD model and Reaxff model.

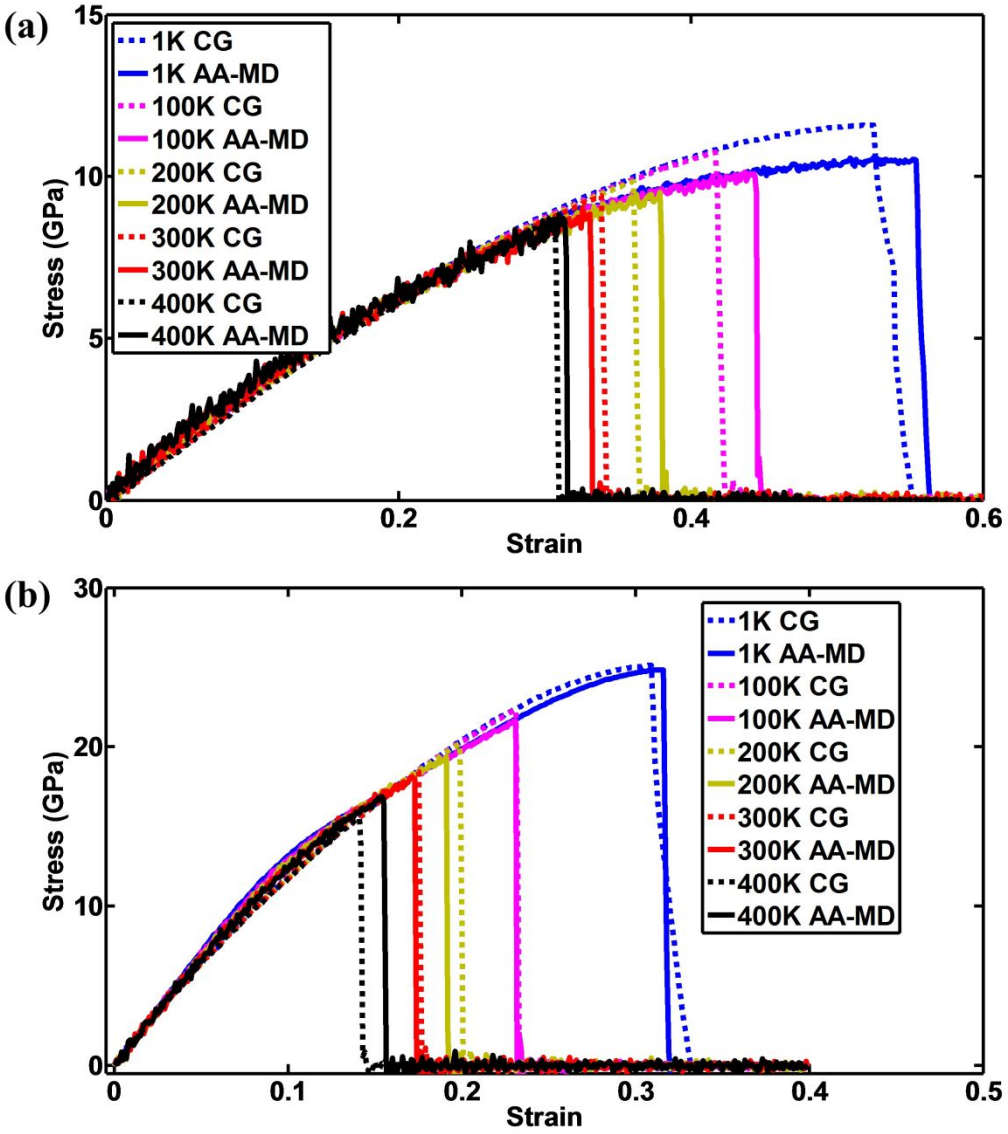

Figure 4. Comparison of stress-strain responses between CG-MD and AA-MD simulations along the (a) armchair direction; (b) zigzag direction.

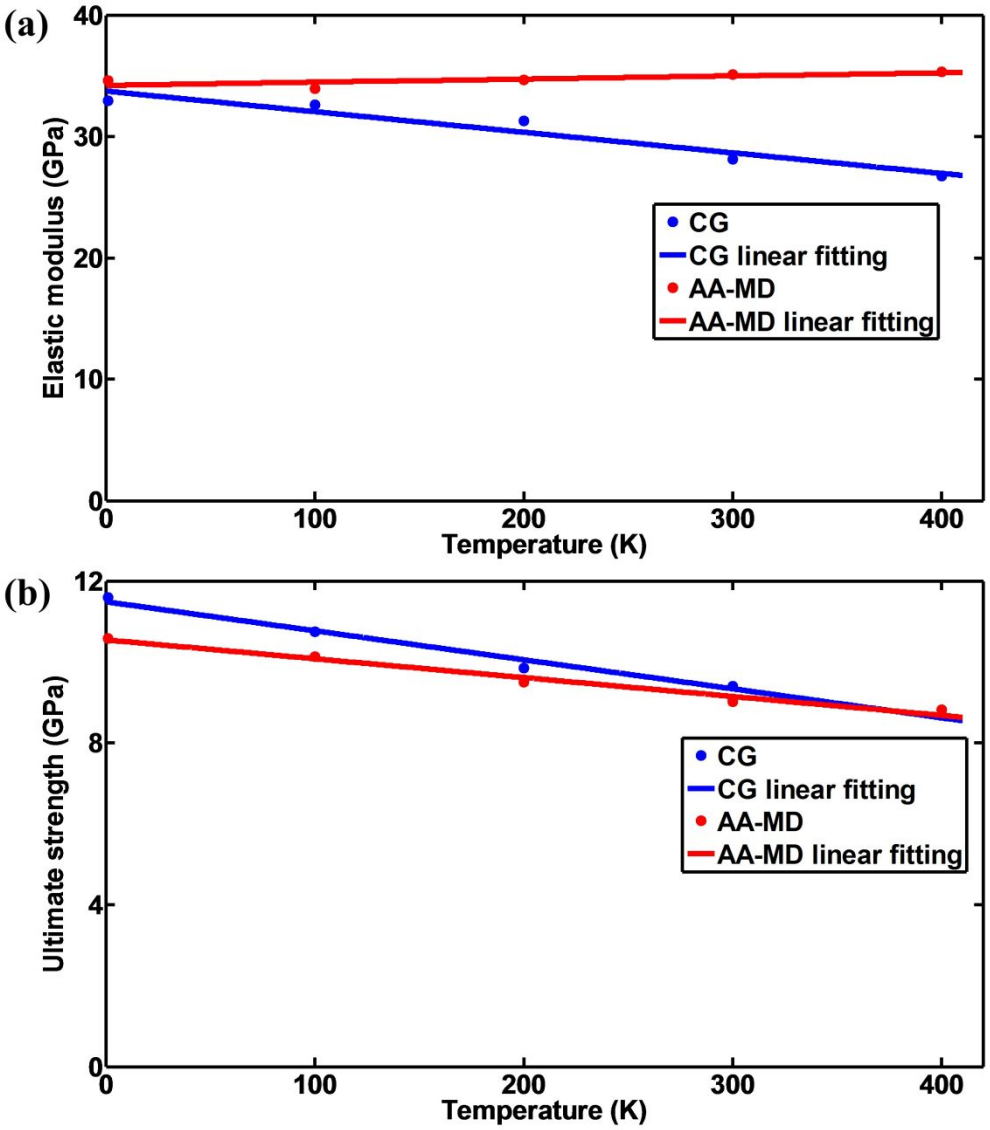

Figure 5. Temperature dependence of mechanical properties (a) Elastic modulus; (b) Ultimate strength (Based on results from uniaxial stretch along armchair direction).

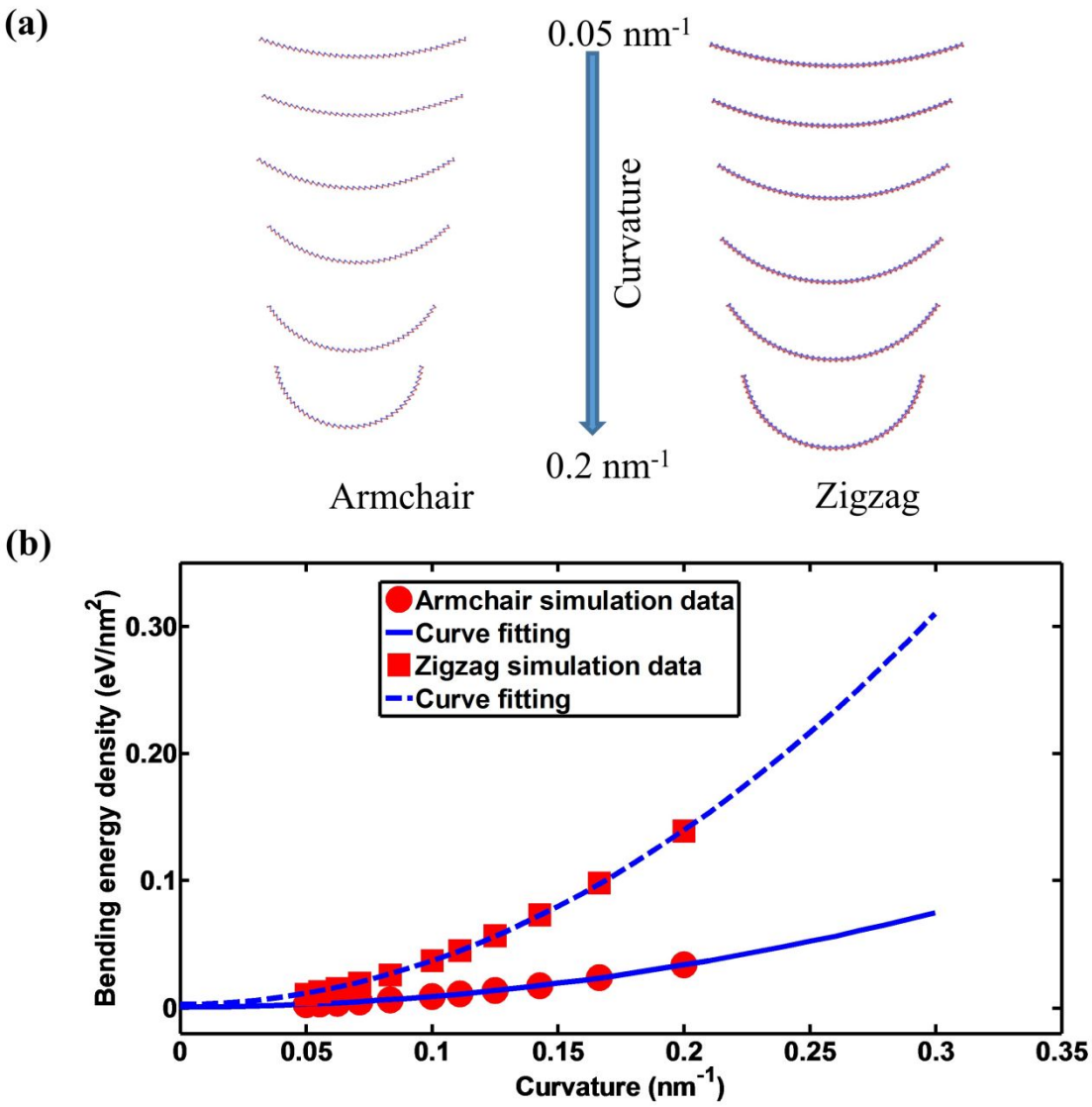

Figure 6. (a) Schematic view of bending test for phosphorene using CG-MD model. (b) Bending energy versus curvature of the phosphorene sheet based on the CG-MD model.

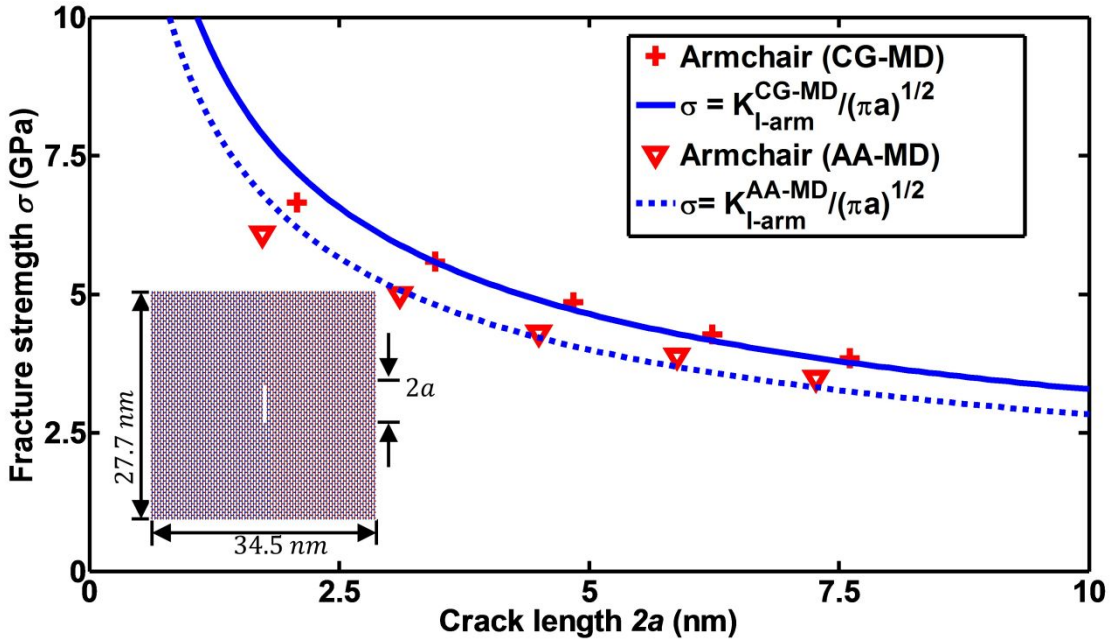

Figure 7. Fracture strength versus crack length for phosphorene sheets with cracks vertical to the armchair direction under tension along armchair direction

References

[1] L. Li, Y. Yu, G.J. Ye, Q. Ge, X. Ou, H. Wu, D. Feng, X.H. Chen, Y. Zhang, Black phosphorus field-effect transistors, Nature Nanotechnology 9 (2014) 372.
[2] H. Liu, A.T. Neal, Z. Zhu, Z. Luo, X. Xu, D. Tománek, P.D. Ye, Phosphorene: An Unexplored 2D Semiconductor with a High Hole Mobility, ACS Nano 8(4) (2014) 4033-4041.
[3] F. Hao, X. Chen, Mechanical properties of phosphorene nanoribbons and oxides, Journal of Applied Physics 118(23) (2015) 234304.
[4] J. Jin-Wu, S.P. Harold, Mechanical properties of single-layer black phosphorus, Journal of Physics D: Applied Physics 47(38) (2014) 385304.
[5] H. Sun, G. Liu, Q. Li, X.G. Wan, First-principles study of thermal expansion and thermomechanics of single-layer black and blue phosphorus, Physics Letters A 380(24) (2016) 2098-2104.
[6] Q. Wei, X. Peng, Superior mechanical flexibility of phosphorene and few-layer black phosphorus, Applied Physics Letters 104(25) (2014) 251915.
[7] H. Xiao, X. Shi, F. Hao, X. Liao, Y. Zhang, X. Chen, Development of a Transferable Reactive Force Field of P/H Systems: Application to the Chemical and Mechanical Properties of Phosphorene, The Journal of Physical Chemistry A 121(32) (2017) 6135-6149.
[8] J.-W. Jiang, H.S. Park, Negative poisson's ratio in single-layer black phosphorus, Nature Communications 5 (2014) 4727.
[9] X. Wei, Z. Meng, L. Ruiz, W. Xia, C. Lee, J.W. Kysar, J.C. Hone, S. Keten, H.D. Espinosa, Recoverable Slippage Mechanism in Multilayer Graphene Leads to Repeatable Energy Dissipation, ACS Nano 10(2) (2016) 1820-1828.
[10] S. Cranford, D. Sen, M.J. Buehler, Meso-origami: Folding multilayer graphene sheets, Applied Physics Letters 95(12) (2009) 123121.
[11] Z. Meng, J. Han, X. Qin, Y. Zhang, O. Balogun, S. Keten, Spalling-like failure by cylindrical projectiles deteriorates the ballistic performance of multi-layer graphene plates, Carbon 126 (2018) 611-619.
[12] J.-J. Shang, Q.-S. Yang, X. Liu, New Coarse-Grained Model and Its Implementation in Simulations of Graphene Assemblies, Journal of Chemical Theory and Computation 13(8) (2017) 3706-3714.
[13] Z.Y. Yang, J.H. Zhao, N. Wei, Temperature-dependent mechanical properties of monolayer black phosphorus by molecular dynamics simulations, Applied Physics Letters 107(2) (2015) 5.
[14] B. Liu, L. Bai, E.A. Korznikova, S.V. Dmitriev, A.W.-K. Law, K. Zhou, Thermal Conductivity and Tensile Response of Phosphorene Nanosheets with Vacancy Defects, The Journal of Physical Chemistry C 121(25) (2017) 13876-13887.
[15] L. Kou, Y. Ma, S.C. Smith, C. Chen, Anisotropic Ripple Deformation in Phosphorene, The Journal of Physical Chemistry Letters 6(9) (2015) 1509-1513.
[16] S. Zhen-Dong, P. Qing-Xiang, D. Zhiwei, J. Jin-Wu, Z. Yong-Wei, Mechanical properties and fracture behavior of single-layer phosphorene at finite temperatures, Journal of Physics D: Applied Physics 48(39) (2015) 395303.
[17] N. Liu, J. Hong, R. Pidaparti, X. Wang, Fracture patterns and the energy release rate of phosphorene, Nanoscale 8(10) (2016) 5728-5736.
[18] B. Lichun, L. Bo, S. Narasimalu, T. Yu, Z. Kun, Nano-friction behavior of phosphorene, Nanotechnology 28(35) (2017) 355704.
[19] N. Liu, J. Hong, X. Zeng, R. Pidaparti, X. Wang, Fracture mechanisms in multilayer phosphorene assemblies: from brittle to ductile, Physical Chemistry Chemical Physics 19(20) (2017) 13083-13092.
[20] L. Ruiz, W. Xia, Z. Meng, S. Keten, A coarse-grained model for the mechanical behavior of multi-layer graphene, Carbon 82 (2015) 103-115.
[21] A.V. Titov, P. Král, R. Pearson, Sandwiched Graphene–Membrane Superstructures, ACS Nano 4(1) (2010) 229-234.

[22] N. Liu, X. Zeng, R. Pidaparti, X. Wang, Tough and strong bioinspired nanocomposites with interfacial cross-links, Nanoscale 8(43) (2016) 18531-18540.
[23] N. Liu, R. Pidaparti, X. Wang, Mechanical Performance of Graphene-Based Artificial Nacres under Impact Loads: A Coarse-Grained Molecular Dynamic Study, Polymers 9(4) (2017) 134.
[24] Z. Meng, A. Singh, X. Qin, S. Keten, Reduced ballistic limit velocity of graphene membranes due to cone wave reflection, Extreme Mechanics Letters 15 (2017) 70-77.
[25] Y. Li, C.B. Abberton, M. Kröger, K.W. Liu, Challenges in Multiscale Modeling of Polymer Dynamics, Polymers 5(2) (2013).
[26] D.D. Hsu, W. Xia, S.G. Arturo, S. Keten, Systematic Method for Thermomechanically Consistent Coarse-Graining: A Universal Model for Methacrylate-Based Polymers, Journal of Chemical Theory and Computation 10(6) (2014) 2514-2527.
[27] D.D. Hsu, W. Xia, S.G. Arturo, S. Keten, Thermomechanically Consistent and Temperature Transferable Coarse-Graining of Atactic Polystyrene, Macromolecules 48(9) (2015) 3057-3068.
[28] E. Brini, V. Marcon, N.F.A. van der Vegt, Conditional reversible work method for molecular coarse graining applications, Physical Chemistry Chemical Physics 13(22) (2011) 10468-10474.
[29] Y. Wang, W.G. Noid, P. Liu, G.A. Voth, Effective force coarse-graining, Physical Chemistry Chemical Physics 11(12) (2009) 2002-2015.
[30] E. Brini, E.A. Algaer, P. Ganguly, C. Li, F. Rodríguez-Ropero, N.F.A. van der Vegt, Systematic coarse-graining methods for soft matter simulations – a review, Soft Matter 9(7) (2013) 2108-2119.
[31] J.-W. Jiang, T. Rabczuk, H.S. Park, A Stillinger–Weber potential for single-layered black phosphorus, and the importance of cross-pucker interactions for a negative Poisson's ratio and edge stress-induced bending, Nanoscale 7(14) (2015) 6059-6068.
[32] L. Minh-Quy, Reactive molecular dynamics simulations of the mechanical properties of various phosphorene allotropes, Nanotechnology 29(19) (2018) 195701.
[33] Z. Meng, R.A. Soler-Crespo, W. Xia, W. Gao, L. Ruiz, H.D. Espinosa, S. Keten, A coarse-grained model for the mechanical behavior of graphene oxide, Carbon 117 (2017) 476-487.
[34] L. Monticelli, S.K. Kandasamy, X. Periole, R.G. Larson, D.P. Tieleman, S.-J. Marrink, The MARTINI Coarse-Grained Force Field: Extension to Proteins, Journal of Chemical Theory and Computation 4(5) (2008) 819-834.
[35] W. Xia, S. Mishra, S. Keten, Substrate vs. free surface: Competing effects on the glass transition of polymer thin films, Polymer 54(21) (2013) 5942-5951.
[36] T. Belytschko, S.P. Xiao, G.C. Schatz, R.S. Ruoff, Atomistic simulations of nanotube fracture, Physical Review B 65(23) (2002) 235430.
[37] J. Jin-Wu, Parametrization of Stillinger–Weber potential based on valence force field model: application to single-layer MoS 2 and black phosphorus, Nanotechnology 26(31) (2015) 315706.
[38] A.C. Eringen, Mechanics of continua, Huntington, NY, Robert E. Krieger Publishing Co., 1980. 606 p. (1980).
[39] S. Appalakondaiah, G. Vaitheeswaran, S. Lebègue, N.E. Christensen, A. Svane, Effect of van der Waals interactions on the structural and elastic properties of black phosphorus, Physical Review B 86(3) (2012) 035105.
[40] P.P. Gillis, Calculating the elastic constants of graphite, Carbon 22(4) (1984) 387-391.
[41] S. Plimpton, Fast Parallel Algorithms for Short-Range Molecular Dynamics, Journal of Computational Physics 117(1) (1995) 1-19.
[42] X.H. Peng, A. Alizadeh, S.K. Kumar, S.K. Nayak, AB INITIO STUDY OF SIZE AND STRAIN EFFECTS ON THE ELECTRONIC PROPERTIES OF Si NANOWIRES, International Journal of Applied Mechanics 01(03) (2009) 483-499.
[43] P. Xihong, T. Fu, L. Paul, Band structure of Si/Ge core–shell nanowires along the [110] direction modulated by external uniaxial strain, Journal of Physics: Condensed Matter 23(11) (2011) 115502.

[44] M.R. Falvo, G.J. Clary, R.M. Taylor Ii, V. Chi, F.P. Brooks Jr, S. Washburn, R. Superfine, Bending and buckling of carbon nanotubes under large strain, Nature 389 (1997) 582.
[45] R.S. Jacobsen, K.N. Andersen, P.I. Borel, J. Fage-Pedersen, L.H. Frandsen, O. Hansen, M. Kristensen, A.V. Lavrinenko, G. Moulin, H. Ou, C. Peucheret, B. Zsigri, A. Bjarklev, Strained silicon as a new electro-optic material, Nature 441 (2006) 199.
[46] P. Logan, X. Peng, Strain-modulated electronic properties of Ge nanowires: A first-principles study, Physical Review B 80(11) (2009) 115322.
[47] Q.-X. Pei, Z.-D. Sha, Y.-Y. Zhang, Y.-W. Zhang, Effects of temperature and strain rate on the mechanical properties of silicene, Journal of Applied Physics 115(2) (2014) 023519.
[48] P. Carbone, H.A.K. Varzaneh, X. Chen, F. Müller-Plathe, Transferability of coarse-grained force fields: The polymer case, The Journal of Chemical Physics 128(6) (2008) 064904.
[49] H.A. Karimi-Varzaneh, P. Carbone, F. Müller-Plathe, Fast dynamics in coarse-grained polymer models: The effect of the hydrogen bonds, The Journal of Chemical Physics 129(15) (2008) 154904.
[50] W.G. Noid, Perspective: Coarse-grained models for biomolecular systems, The Journal of Chemical Physics 139(9) (2013) 090901.
[51] P. Depa, C. Chen, J.K. Maranas, Why are coarse-grained force fields too fast? A look at dynamics of four coarse-grained polymers, The Journal of Chemical Physics 134(1) (2011) 014903.
[52] J.P. Garrahan, D. Chandler, Coarse-grained microscopic model of glass formers, Proceedings of the National Academy of Sciences 100(17) (2003) 9710-9714.
[53] C.L. Phillips, J.A. Anderson, S.C. Glotzer, Pseudo-random number generation for Brownian Dynamics and Dissipative Particle Dynamics simulations on GPU devices, Journal of Computational Physics 230(19) (2011) 7191-7201.
[54] N. Grønbech-Jensen, O. Farago, A simple and effective Verlet-type algorithm for simulating Langevin dynamics, Molecular Physics 111(8) (2013) 983-991.
[55] D. Verma, B. Hourahine, T. Frauenheim, R.D. James, T. Dumitrică, Directional-dependent thickness and bending rigidity of phosphorene, Physical Review B 94(12) (2016) 121404.
[56] Z. Hao-Yu, J. Jin-Wu, Elastic bending modulus for single-layer black phosphorus, Journal of Physics D: Applied Physics 48(45) (2015) 455305.
[57] A.J. Mannix, Z. Zhang, N.P. Guisinger, B.I. Yakobson, M.C. Hersam, Borophene as a prototype for synthetic 2D materials development, Nature Nanotechnology 13(6) (2018) 444-450.
[58] P. Zhang, L. Ma, F. Fan, Z. Zeng, C. Peng, P.E. Loya, Z. Liu, Y. Gong, J. Zhang, X. Zhang, P.M. Ajayan, T. Zhu, J. Lou, Fracture toughness of graphene, Nature Communications 5 (2014) 3782.
[59] M.J.B. Moura, M. Marder, Tearing of free-standing graphene, Physical Review E 88(3) (2013) 032405.
[60] Z. Meng, M.A. Bessa, W. Xia, W. Kam Liu, S. Keten, Predicting the Macroscopic Fracture Energy of Epoxy Resins from Atomistic Molecular Simulations, Macromolecules 49(24) (2016) 9474-9483.
[61] J. Rottler, S. Barsky, M.O. Robbins, Cracks and Crazes: On Calculating the Macroscopic Fracture Energy of Glassy Polymers from Molecular Simulations, Physical Review Letters 89(14) (2002) 148304.
[62] D. Midtvedt, A. Croy, Valence-force model and nanomechanics of single-layer phosphorene, Physical Chemistry Chemical Physics 18(33) (2016) 23312-23319.